Array Synthesis With Low Sidelobe Level Using Two-Way Array Factor: A Mixed-Integer Programming Approach

LINGRUI LI
XUEJING ZHANG, Member, IEEE
YUANYUAN ZHENG
ZISHU HE, Senior Member, IEEE
University of Electronic Science and Technology of China, Chengdu, China

In this article, we consider the array synthesis with low sidelobe level using two-way array factor (AF), which is defined as the product of the factors in transmit and receive AFs. Utilizing the integer modeling techniques, we reformulate and simplify the nonconvex constraint on sidelobe level, and the coupled variables are linearized according to the characteristics of binary vectors. This allows us to derive a mixed-integer programming (MIP) two-way array synthesis formulation with sidelobe suppression, which can be solved by MIP solvers. Compared to existing algorithms, which rely on uniform transmit array or complex excitation distribution, the proposed algorithm yields more flexible arrays with uniform excitation. Moreover, the main lobe width of the two-way AF can be added to the constraints and adjusted as desired at the cost of an acceptable longer running time. In addition, our algorithm can be extended to more scenarios due to the flexibility of the two-way array structure. Representative simulations are provided to demonstrate the effectiveness and superiority of the proposed algorithm in various scenarios.

Received 30 April 2025; revised 16 September 2025; accepted 8 October 2025. Date of publication 13 October 2025; date of current version 7 January 2026.

DOI. No. 10.1109/TAES.2025.3620278

Refereeing of this contribution was handled by Ali Cafer Gurbuz.

This work was supported in part by the National Nature Science Foundation of China under Grant 62101101, in part by the Sichuan Science and Technology Program under Grant 24NSFSC1433, and in part by the Peng Cheng Shang Xue Education Fund under Grant XY2021602.

Authors' address: Lingrui Li, Xuejing Zhang, Yuanyuan Zheng, and Zishu He are with the School of Information and Communication Engineering, University of Electronic Science and Technology of China, Chengdu 611731, China, E-mail: (202321010741@std.uestc.edu.cn; xjzhang7@163.com; 1005427506@qq.cn; zshe@uestc.edu.cn). *(Corresponding author: Xuejing Zhang.)*

I. INTRODUCTION

The presence of unwanted sidelobes decreases radiation efficiency [1], making low peak sidelobe level (PSL) a critical concern in antenna array design, especially for applications, such as radar and communication systems. Due to the importance of reducing PSL in antenna arrays, numerous techniques have been proposed over the past decades. Typically, antenna arrays can reduce PSL by designing amplitude and phase excitation [2], [3], [4], [5] or element positions [6], [7], [8], [9], [10], [11], [12], [13], as well as various recent methods, such as partially controlled elements [14], clustered subarrays [15], and compressive sensing arrays [16]. Commonly, only the PSL of the transmit beam or the receive beam is considered, depending on the specific application. In radar systems, the transmit antenna and the receive antenna can be shared, which provides benefits in terms of simplicity and efficiency. The shared transmit–receive antenna leads to the concept of two-way array factor (AF) [17], [18], which comprehensively considers both the transmit beam and the receive beam. Various two-way array systems have attracted research works, such as colocated MIMO radar [19], [20] and full-duplex communication arrays [21], [22].

Over the past few years, a number of sidelobe reduction strategies have been proposed based on the concept of two-way AF [23], [24], [25], [26], [27], [28], [29], [30], [31], [32], [33], [34]. Brock [23] investigated three different methods for sidelobe suppression, including the Taylor-weighted transmit array, split and steering uniformly excited transmit array, and quadratic phase adjusted uniform transmit array. The receive arrays in the above-mentioned methods are all Taylor-weighted. However, the transmitted power loses to concentrate over the main beam effectively. The introduction of two/three-weighted amplitude distribution for antenna arrays is also a way by which sidelobe suppression can be achieved in linear or rectangular arrays [24], [25], [26], [27], [28], and circular arrays [29]. The number of elements excited with higher weights or the relation between the sizes of transmit and receive arrays was found from various test sets, and the arrays were accordingly designed. Nevertheless, only approximate suboptimal solutions can be obtained. In addition, all the abovementioned methods would cause a large dynamic range ratio (DRR), which is defined as the proportion between the maximum and minimum amplitude of element excitation. Excessive DRR causes the RF components to exceed the linear working interval, and hardware needs to be modified to avoid uncontrollable distortion, hence being costly and complicated.

To reduce the DRR in two-way arrays, low sidelobe two-way AFs have been designed with uniformly weighted elements utilizing uniform transmit and thinned receive arrays [29], [30], [31], [32], [33], [34]. The authors of [29], [30], and [31] achieved the uniformly thinning of the receive array; the determination of the thinned receive array size is by matching the first peak sidelobe of the transmit AF to the

first null point of the receive AF in linear, rectangular, or circular arrays. On the basis of this method, a nonuniform receive array arrangement is designed in [32] by introducing the extended coprime array structure. However, the above methods can only obtain a suboptimal solution. As an improvement of the above algorithms, in order to obtain the optimal receive array structure, the genetic algorithm in receive elements selection is utilized in [33] and [34]. The idea of receive elements selection improves the degree of freedom in two-way array synthesis to some extent, yet still loses to achieve the flexibility of the transmit array structure.

All the aforementioned strategies are limited to a uniform transmit array structure. Therefore, the number of elements is not flexible to specify under the condition of determined array aperture, and the main lobe width (MLW) of the obtained two-way AF is inconvenient to adjust. In this article, drawing inspiration from the two-way AF sidelobe suppression in previous works, we propose a mixed-integer programming (MIP) algorithm. We set up the scheme of selecting the transmit and receive arrays from the original uniform array and provide uniform excitation; the flexibility of the array structure is therefore guaranteed. By introducing binary variables and using the integer modeling techniques, the PSL suppression problem with the required MLW can ultimately be solved as an MIP problem by MIP solvers. Compared to existing algorithms, the proposed algorithm obtains a satisfactory PSL suppression effect with uniform excitation, and the two-way AF can be designed according to the required MLW. Moreover, our algorithm can be extended to more scenarios due to the flexibility of the two-way array structure. Representative simulations are conducted to show the effectiveness and superiority of the proposed algorithm.

The rest of this article is organized as follows. In Section II, the model of two-way AF is described and the array synthesis problem using two-way AF is elicited. The MIP algorithm for the PSL minimizing problem of the two-way AF is presented in Section III. In Section IV, two extensions of the MIP algorithm for the array synthesis problem with low PSL constraint using two-way AF are introduced. Representative simulations are presented in Section V. Finally, Section VI concludes this article.

II. PROBLEM FORMULATION

Consider a transmit array composed of N_t elements lying along the x-direction at arbitrary but known locations p_m with $m = 1, 2, \ldots, N_t$. Contained in the transmit array, N_r elements ($N_r \le N_t$) located at q_n with $n = 1, 2, \ldots, N_r$ are used as the receive array simultaneously. The transmit AF is written as

$$\mathrm{AF}_t(\theta) = \sum_{m=1}^{N_t} t_m e^{-j\frac{2\pi}{\lambda}p_m \sin\theta} = \boldsymbol{t}^T \boldsymbol{a}_t(\theta) \tag{1}$$

while the receive AF is written as

$$\mathrm{AF}_r(\theta) = \sum_{n=1}^{N_r} r_n e^{j\frac{2\pi}{\lambda}q_n \sin\theta} = \boldsymbol{r}^T \boldsymbol{a}_r(\theta) \tag{2}$$

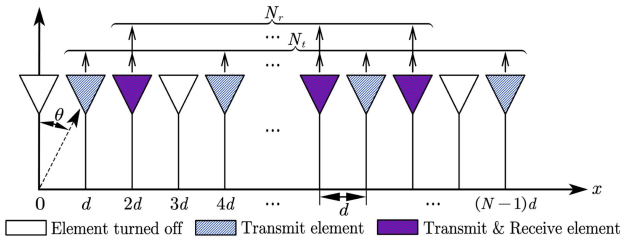

Fig. 1. Example of a two-way array.

where $\boldsymbol{t} = [t_1, t_2, \ldots, t_{N_t}]^T$ and $\boldsymbol{r} = [r_1, r_2, \ldots, r_{N_r}]^T$ are the transmit excitation vector and the receive excitation vector, respectively. $(\cdot)^T$ denotes the transpose operation, and $\boldsymbol{a}_t(\theta)$ and $\boldsymbol{a}_r(\theta)$ are the steering vectors of the transmit array and receive array, respectively, defined as

$$\boldsymbol{a}_t(\theta) = [e^{-j\frac{2\pi}{\lambda}p_1 \sin\theta}, e^{-j\frac{2\pi}{\lambda}p_2 \sin\theta}, \ldots, e^{-j\frac{2\pi}{\lambda}p_{N_t} \sin\theta}]^T \tag{3}$$

$$\boldsymbol{a}_r(\theta) = [e^{j\frac{2\pi}{\lambda}q_1 \sin\theta}, e^{j\frac{2\pi}{\lambda}q_2 \sin\theta}, \ldots, e^{j\frac{2\pi}{\lambda}q_{N_r} \sin\theta}]^T \tag{4}$$

where λ stands for the wavelength and θ denotes the azimuth angle from broadside.

Multiplying the transmit and receive AFs results in the two-way AF

$$\mathrm{AF}_2(\theta) = \mathrm{AF}_t(\theta) \cdot \mathrm{AF}_r(\theta). \tag{5}$$

The synthesis target is to improve the performance of the two-way AF by optimizing the positions of transmit and receive antennas. To address the problem, a uniform receive array thinning (URAT) method is introduced in [31], and a genetic receive array thinning (GRAT) algorithm is introduced in [33], which is limited to a uniform transmit array structure and an inflexible number of elements, and the sidelobe range of the obtained two-way AF is changeless. Sahalos [24] introduced a two-weighted amplitude distribution method with a thinned receive array (TWTR), while Rajender et al. [28] utilized a complete receive array (TWCR). In addition to the above defects, the complex excitation distribution also increased the hardware complexity. Therefore, we propose a new formulation of two-way array synthesis with low sidelobe level via MIP.

III. MIP ALGORITHM

In this section, we describe a new modeling approach for the element position optimization problem, and an MIP algorithm for the PSL minimizing problem of the two-way AF is proposed. The proposed algorithm guarantees the flexibility of the array and the elements are uniformly excited.

A. Modeling of Element Position Optimization Problem

In order to yield more flexible array structure, it is specified to select the elements from a uniform N-element array with interelement spacing d. N_t elements are selected as the transmit array (other elements are turned OFF), while N_r elements contained in the transmit array are selected simultaneously as the receive array. An example is given as reference in Fig. 1. The N_t-dimensional transmit vector $\boldsymbol{t}$ and the N_r-dimensional receive vector $\boldsymbol{r}$ can be therefore

expanded to N-dimensional and should satisfy

$$\begin{cases} t_n = 1,\ r_n = 1 & \text{element transmit and receive} \\ t_n = 1,\ r_n = 0 & \text{element transmit only} \\ t_n = 0,\ r_n = 0 & \text{element turned off} \end{cases} \tag{6}$$

and the l_0 norms of $\boldsymbol{t}$ and $\boldsymbol{r}$ should be N_t and N_r, respectively. Note that $t_m = 1$ or $r_n = 1$ not only represents that the element is selected but also implies that the elements turned ON are uniformly excited. Since the receive array is selected from the transmit array, when a certain bit of $\boldsymbol{t}$ is equal to 1, the same bit of $\boldsymbol{r}$ can be equal to either 0 or 1, and when a certain bit of $\boldsymbol{t}$ is equal to 0, the same bit of $\boldsymbol{r}$ must be equal to 0.

Take the focused two-way array synthesis problem for example, the minimization of PSL is taken as the synthesis target. Since the numbers of transmit and receive elements have been determined and the weights are uniform, the main lobe of the two-way AF directed to $\theta_0 = 0^\circ$ is assured and the level is a constant, i.e., $N_t N_r$. The problem can be expressed as

$$\min_{\boldsymbol{t},\boldsymbol{r},\rho} \quad \rho \tag{7a}$$

$$\text{s.t.} \quad |\boldsymbol{t}^T \boldsymbol{a}_t(\theta_s)\boldsymbol{a}_r^T(\theta_s)\boldsymbol{r}| \le \rho,\ \theta_s \in \Theta_S \tag{7b}$$

$$\mathbf{1}_N^T \boldsymbol{t} = N_t \tag{7c}$$

$$\mathbf{1}_N^T \boldsymbol{r} = N_r \tag{7d}$$

$$\boldsymbol{r} \preceq \boldsymbol{t} \tag{7e}$$

$$\boldsymbol{t}, \boldsymbol{r} \in \{0, 1\}^N \tag{7f}$$

where ρ represents the PSL, and Θ_S denotes the sidelobe region, where $\mathbf{1}_k$ denotes a k-dimensional all-one column vector. Elements in $\boldsymbol{t}$ and $\boldsymbol{r}$ can only take the values of 0 or 1 as indicated in (7f). In (7c) and (7d), the numbers of elements selected by the transmit array and receive array are constrained. It is implicated in (7e) that when a certain bit of $\boldsymbol{t}$ is equal to 0, the same bit of $\boldsymbol{r}$ must be equal to 0, i.e., the receive elements are selected from the transmit array. It should be noted that the beampattern synthesis problem formulation can be completed similarly when utilizing non-isotropic elements and introducing element patterns. It only requires to multiply the element patterns to the AF and add necessary constraints.

REMARK 1: In the case of uniform excitation, as the obtained $\boldsymbol{t}$ and $\boldsymbol{r}$ are real-valued, the main lobe of the synthesized two-way AF can only direct to 0°. On this basis, by taking Hadamard product of the obtained $\boldsymbol{t}$ and $\boldsymbol{r}$ with Vandermonde phase adjustment vectors related to the desired main lobe direction, beam translation, i.e., beam scanning, can be achieved. It should be noted that since beam translation would cause the grating lobe problem, the sidelobe region should be appropriately widened in the form of the sine value.

B. Two-Way Array Synthesis Via MIP

The main challenge for the optimization problem (7) lies in the product form of two optimization variables in constraint (7b), which makes solving the problem very complicated. Before addressing the two-way array synthesis problem (7), to handle the intricate constraint (7b), it is essential to observe the following equality:

$$\boldsymbol{t}^T \boldsymbol{a}_t(\theta_s)\boldsymbol{a}_r^T(\theta_s)\boldsymbol{r} = (\boldsymbol{r} \otimes \boldsymbol{t})^T \text{vec}[\boldsymbol{a}_t(\theta_s)\boldsymbol{a}_r^T(\theta_s)] \tag{8}$$

where we have $\text{vec}(\boldsymbol{B}_1\boldsymbol{B}_2\boldsymbol{B}_3) = (\boldsymbol{B}_3^T \otimes \boldsymbol{B}_1)\text{vec}(\boldsymbol{B}_2)$ in which $\boldsymbol{B}_1$, $\boldsymbol{B}_2$, and $\boldsymbol{B}_3$ are multiplicable matrices, $\otimes$ denotes the Kronecker product, and $\text{vec}(\cdot)$ represents vectorization.

Then, by introducing new optimization variable $\boldsymbol{v} \triangleq \boldsymbol{r} \otimes \boldsymbol{t}$, where $\boldsymbol{v} = [v_1, v_2, \ldots, v_{N^2}]^T$, problem (7) can be readily re-expressed as

$$\min_{\boldsymbol{t},\boldsymbol{r},\boldsymbol{v},\rho} \quad \rho \tag{9a}$$

$$\text{s.t.} \quad |\boldsymbol{v}^T \text{vec}[\boldsymbol{a}_t(\theta_s)\boldsymbol{a}_r^T(\theta_s)]| \le \rho,\ \theta_s \in \Theta_S \tag{9b}$$

$$\mathbf{1}_N^T \boldsymbol{t} = N_t \tag{9c}$$

$$\mathbf{1}_N^T \boldsymbol{r} = N_r \tag{9d}$$

$$\boldsymbol{r} \preceq \boldsymbol{t} \tag{9e}$$

$$\boldsymbol{v} = \boldsymbol{r} \otimes \boldsymbol{t} \tag{9f}$$

$$\boldsymbol{t}, \boldsymbol{r} \in \{0, 1\}^N. \tag{9g}$$

Through the aforementioned operations, the complicated constraint (7b) has been transformed into the form of a tractable constraint (9b). However, it should be noted that the operations introduce a new intricate constraint (9f) to the optimization problem and need to be processed.

Considering the definition of Kronecker product, on the condition of $1 \le m, n \le N$ (this condition is guaranteed in the following text), each element in $\boldsymbol{v}$ is equal to the product of the elements in $\boldsymbol{t}$ and $\boldsymbol{r}$ of the corresponding bits

$$v_{N(n-1)+m} = t_m \cdot r_n. \tag{10}$$

Since $\boldsymbol{t}$ and $\boldsymbol{r}$ are binary vectors, $\boldsymbol{v}$ should be a binary vector, and according to the properties, an equivalent replacement of (10) can be written as

$$t_m + r_n - 1 \le v_{N(n-1)+m} \le t_m \tag{11a}$$

$$t_m + r_n - 1 \le v_{N(n-1)+m} \le r_n \tag{11b}$$

$$v_{N(n-1)+m} \in \{0, 1\} \tag{11c}$$

which assures that $v_{N(n-1)+m} = 0$ when $t_m = 0$ or $r_n = 0$ and $v_{N(n-1)+m} = 1$ when $t_m = r_n = 1$. Therefore, problem (9) can be rewritten as follows:

$$\min_{\boldsymbol{t},\boldsymbol{r},\boldsymbol{v},\rho} \quad \rho \tag{12a}$$

$$\text{s.t.} \quad |\boldsymbol{v}^T \text{vec}[\boldsymbol{a}_t(\theta_s)\boldsymbol{a}_r^T(\theta_s)]| \le \rho,\ \theta_s \in \Theta_S \tag{12b}$$

$$\mathbf{1}_N^T \boldsymbol{t} = N_t \tag{12c}$$

$$\mathbf{1}_N^T \boldsymbol{r} = N_r \tag{12d}$$

$$\boldsymbol{r} \preceq \boldsymbol{t} \tag{12e}$$

$$\boldsymbol{v} \preceq \boldsymbol{r} \otimes \mathbf{1}_N \tag{12f}$$

$$\boldsymbol{v} \preceq \mathbf{1}_N \otimes \boldsymbol{t} \tag{12g}$$

$$\boldsymbol{v} \succeq \boldsymbol{r} \otimes \mathbf{1}_N + \mathbf{1}_N \otimes \boldsymbol{t} - \mathbf{1}_{N^2} \tag{12h}$$

$$\boldsymbol{v} \in \{0, 1\}^{N^2} \tag{12i}$$

$$\boldsymbol{t}, \boldsymbol{r} \in \{0, 1\}^N \tag{12j}$$

where (12f)–(12i) is an equivalent replacement of constraint (9f); the equivalence of the replacement is proved as described above. The problem (12) is an MIP problem, where some variables (see vectors $\boldsymbol{t}$, $\boldsymbol{r}$, and $\boldsymbol{v}$) can only take on integer values, while others (see ρ) can take on continuous values. The model is tractable and the optimal solution can be found theoretically. Note that in large-scale problems, suboptimal solutions can be considered to reduce running time. In fact, we can solve problem (12) using MIP solvers, such as GUROBI [35] and CPLEX [36].

REMARK 2: In fact, the running time of the above algorithm can be reduced by reducing the integer variables. It is not difficult to find that the inequality constraints (11a) and (11b) can already guarantee that $v_{N(n-1)+m}$ takes values correctly when either $t_m = 1$ or $r_n = 1$, just an extra constraint to guarantee $v_{N(n-1)+m} = 0$ when $t_m = r_n = 0$ is required. Therefore, to reduce the running time, it is recommended to convert (11) into an equivalent form

$$t_m + r_n - 1 \le v_{N(n-1)+m} \le t_m \tag{13a}$$
$$t_m + r_n - 1 \le v_{N(n-1)+m} \le r_n \tag{13b}$$
$$v_{N(n-1)+m} \ge 0 \tag{13c}$$

in which $v_{N(n-1)+m}$ is unnecessary to be constrained as an integer variable and all constraints are re-expressed to linear form, which benefits in reducing algorithm running time. That is, (12i) can be converted to the following form:

$$\boldsymbol{v} \succeq \boldsymbol{0}_{N^2} \tag{14}$$

where $\boldsymbol{0}_k$ denotes a k-dimensional all-zero column vector.

IV. MIP ALGORITHM FOR EXTENDED SCENARIOS

Utilizing the above-mentioned MIP algorithm, the PSL of the two-way AF can be minimized while the numbers of transmit and receive elements are determined. On this basis, under the condition of the determined PSL constraint of the two-way AF, many extensions of the problem can also be handled. We will give two examples in this section.

A. Minimize the Number of Transmit Elements

In order to achieve the reduction of cost, power consumption, and the simplification of the feeding network, the synthesis of two-way arrays with minimum number of elements turned ON is significant, which is equivalent to minimize the number of elements N_t selected as the transmit array. Unlike the upper section, since N_t and N_r are variables to be solved, the main lobe level is no longer constant, and the PSL should be constrained by limiting the ratio of sidelobe level and main lobe level. In order to minimize the number of transmit elements while constraining the PSL below a certain value ρ, the problem can be expressed as

$$\min_{\boldsymbol{t},\boldsymbol{r}} \ \boldsymbol{1}_N^T \boldsymbol{t} \tag{15a}$$
$$\text{s.t.} \ \frac{|\boldsymbol{t}^T \boldsymbol{a}_t(\theta_s)\boldsymbol{a}_r^T(\theta_s)\boldsymbol{r}|}{|\boldsymbol{t}^T \boldsymbol{a}_t(\theta_0)\boldsymbol{a}_r^T(\theta_0)\boldsymbol{r}|} \le \rho, \ \theta_s \in \Theta_S \tag{15b}$$
$$\boldsymbol{1}_N^T \boldsymbol{r} \ge 1 \tag{15c}$$
$$\boldsymbol{r} \preceq \boldsymbol{t} \tag{15d}$$
$$\boldsymbol{t}, \boldsymbol{r} \in \{0, 1\}^N. \tag{15e}$$

Combining constraints (15c) and (15d), it can be assured that the denominator in (15b) is not zero. It can be seen that (15b) is a complicated constraint and contains a fractional form.

By utilizing (8), taking operations similar to the previous section, problem (15) can be re-expressed as the following form:

$$\min_{\boldsymbol{t},\boldsymbol{r},\boldsymbol{v}} \ \boldsymbol{1}_N^T \boldsymbol{t} \tag{16a}$$
$$\text{s.t.} \ |\boldsymbol{v}^T \text{vec}[\boldsymbol{a}_t(\theta_s)\boldsymbol{a}_r^T(\theta_s)]| \le \rho \boldsymbol{1}_{N^2}^T \boldsymbol{v}, \ \theta_s \in \Theta_S \tag{16b}$$
$$\boldsymbol{1}_N^T \boldsymbol{r} \ge 1 \tag{16c}$$
$$\boldsymbol{r} \preceq \boldsymbol{t} \tag{16d}$$
$$\boldsymbol{v} \preceq \boldsymbol{r} \otimes \boldsymbol{1}_N \tag{16e}$$
$$\boldsymbol{v} \preceq \boldsymbol{1}_N \otimes \boldsymbol{t} \tag{16f}$$
$$\boldsymbol{v} \succeq \boldsymbol{r} \otimes \boldsymbol{1}_N + \boldsymbol{1}_N \otimes \boldsymbol{t} - \boldsymbol{1}_{N^2} \tag{16g}$$
$$\boldsymbol{v} \succeq \boldsymbol{0}_{N^2} \tag{16h}$$
$$\boldsymbol{t}, \boldsymbol{r} \in \{0, 1\}^N \tag{16i}$$

where the fractional form of (15b) is replaced by a tractable constraint (16b). Through the above operations, the problem of minimizing the number of transmit elements is transformed into the MIP problem (16) and can be solved by MIP solvers.

B. Maximize the Min-Spacing Between Transmit Elements

To mitigate the mutual coupling effect between antennas, it is crucial to increase the min-spacing between transmit elements while constraining the PSL below a certain value ρ. On the condition of $1 \le m < n \le N$ (this condition is guaranteed in the following text), it can be easily found that the spacing between the mth element and the nth element is $\delta_{m,n} = d(n-m)$. Due to the min-spacing is the largest value not greater than the spacing between any two transmit elements, by introducing a new variable l, the min-spacing can be expressed as the optimal value of the following problem:

$$\max_{l} \ l \quad \text{s.t.} \ d(n-m) \ge l, \ \text{if} \ t_m = t_n = 1. \tag{17}$$

However, since the locations of the transmit elements cannot be predetermined, it is critical to filter out and constrain the spacing between transmit elements, which can be achieved by introducing a sufficiently large constant γ. The constraint in (17) can be re-expressed as

$$d(n-m) + \gamma(2 - t_m - t_n) \ge l \tag{18}$$

where the choice of γ can be specifically selected from the range $\gamma > d(N-1)$. It is not difficult to find that when $t_m = t_n = 1$, the upper formula is equivalent to the constraint in (17). Otherwise, the constraint would have no effect on the problem. The constraint (18) can be rewritten in the form

of a matrix to achieve a more compact form as follows:

$$d\boldsymbol{H}\boldsymbol{g} + 2\gamma \mathbf{1}_{\frac{N(N-1)}{2}} - \gamma|\boldsymbol{H}|\boldsymbol{t} \succeq l\mathbf{1}_{\frac{N(N-1)}{2}} \tag{19}$$

where the N-dimensional vector $\boldsymbol{g} = [1, 2, \ldots, N]^T$, and the $N(N-1)/2 \times N$-dimensional matrix $\boldsymbol{H}$ is defined as $\boldsymbol{H} \triangleq [\boldsymbol{H}_1{}^T, \boldsymbol{H}_2{}^T, \ldots, \boldsymbol{H}_{N-1}{}^T]^T$, where $\boldsymbol{H}_i$ is an $(N-i) \times N$-dimensional matrix defined as

$$\boldsymbol{H}_i \triangleq [\mathbf{0}_{(N-i)\times(i-1)}, -\mathbf{1}_{N-i}, \boldsymbol{E}_{N-i}], \quad i = 1, 2, \ldots, N-1 \tag{20}$$

where $\mathbf{0}_{k_1\times k_2}$ denotes a $k_1 \times k_2$-dimensional all-zero matrix and being an empty matrix when $k_2 = 0$, and $\boldsymbol{E}_k$ represents the identity matrix of dimension k.

On the basis of the aforementioned, taking operations similar to the previous section utilizing (8), the problem can be rewritten as follows:

$$\max_{\boldsymbol{t},\boldsymbol{r},\boldsymbol{v},l} \quad l \tag{21a}$$

$$\text{s.t.} \quad |\boldsymbol{v}^T \text{vec}[\boldsymbol{a}_t(\theta_s)\boldsymbol{a}_r^T(\theta_s)]| \le \rho \mathbf{1}_{N^2}^T \boldsymbol{v},\ \theta_s \in \Theta_S \tag{21b}$$

$$d\boldsymbol{H}\boldsymbol{g} + 2\gamma \mathbf{1}_{\frac{N(N-1)}{2}} - \gamma|\boldsymbol{H}|\boldsymbol{t} \succeq l\mathbf{1}_{\frac{N(N-1)}{2}} \tag{21c}$$

$$\mathbf{1}_N^T \boldsymbol{r} \ge 1 \tag{21d}$$

$$\boldsymbol{r} \preceq \boldsymbol{t} \tag{21e}$$

$$\boldsymbol{v} \preceq \boldsymbol{r} \otimes \mathbf{1}_N \tag{21f}$$

$$\boldsymbol{v} \preceq \mathbf{1}_N \otimes \boldsymbol{t} \tag{21g}$$

$$\boldsymbol{v} \succeq \boldsymbol{r} \otimes \mathbf{1}_N + \mathbf{1}_N \otimes \boldsymbol{t} - \mathbf{1}_{N^2} \tag{21h}$$

$$\boldsymbol{v} \succeq \mathbf{0}_{N^2} \tag{21i}$$

$$\boldsymbol{t}, \boldsymbol{r} \in \{0, 1\}^N \tag{21j}$$

where the min-spacing constraint (21c) is tractable. The problem of maximizing the min-spacing between transmit elements is expressed as the MIP problem (21) through the above operations and can be solved by MIP solvers.

REMARK 3: Note that all the above-mentioned scenarios can be extended to a planar array form. Take maximizing the min-spacing between transmit elements as an example, consider a 2-D rectangular planar array with M and N isotropic antennas in the x- and y-directions, and the interelement spacings are d_x and d_y, respectively. The MN-dimensional transmit excitation vector of the planar array is defined as $\boldsymbol{t} = [t_{1,1}, t_{2,1}, \ldots, t_{M,1}, \ldots, t_{1,N}, t_{2,N}, \ldots, t_{M,N}]^T$. Except for transforming the various vectors into 2-D forms accordingly, the min-spacing constraint (21c) should be modified to a 2-D form as follows:

$$\|\boldsymbol{z}(n) - \boldsymbol{z}(m)\|_2 + \gamma(2 - t_m - t_n) \ge l, \quad 1 \le m < n \le MN \tag{22}$$

where $\|\cdot\|_2$ denotes the l_2 norm, γ can be specifically selected from the range $\gamma > \|[d_x(M-1), d_y(N-1)]\|_2$, and $\boldsymbol{z}(i)$ stands for the position coordinate of the ith element defined as

$$\boldsymbol{z}(i) = \left[d_x \left(i - 1 - M \left\lfloor \frac{i-1}{M} \right\rfloor \right), d_y \left\lfloor \frac{i-1}{M} \right\rfloor \right], \quad 1 \le i \le MN \tag{23}$$

where $\lfloor\cdot\rfloor$ stands for the round down operation. The problem can finally be solved similarly as the previous ones.

V. NUMERICAL RESULTS

To demonstrate the effectiveness and superiority of the proposed algorithm, representative simulations are provided in various scenarios in this section. The URAT method in [31], the GRAT method in [33], the TWTR method in [24], the TWCR method in [28], and the classic Chebyshev window (ChebW) method are tested for comparison if applicable. In this article, we define MLW as the width of the nonconstrained angle range. In our simulations, the proposed MIP models are solved by GUROBI [35]. Mutual coupling effect is taken into consideration in the case of element spacing less than $\lambda/2$; following the coupled model established in [37], the channel coupling level is set as $\xi = 0.3$. Full-wave simulations are conducted with dipole antennas using the full-wave simulation toolbox, operating at a center frequency of 2.5 GHz.

In order to ensure the fairness of the comparison simulations, we ensure that the array aperture of each algorithm is set to be the same. The array structure of the contrast methods are performed as described below. The transmit array is uniformly distributed at $\lambda/2$ spacing within the aperture in all contrast methods. The URAT and GRAT methods ensure uniformly excited, and the receive array in URAT is uniformly thinned while that in GRAT is thinned by a genetic algorithm, following the condition $N_t \approx 1.4N_r$. The receive array in TWTR is uniformly thinned at a ratio of $N_t \approx 1.33N_r$ and the DRR is 2. Neither TWCR nor ChebW requires a thinned receive array, and the obtained DRR is 2.17 in TWCR. The AFs depicted in all figures are normalized.

A. PSL Minimization

In the first example, we perform simulations of the scenario that minimizes the PSL with determined element numbers in the transmit array and receive array.

1) *Two-Way AF Comparison:* Various algorithms are simulated to study the performance of the proposed algorithm in PSL minimization. In the proposed algorithm, the element numbers of the arrays are constrained the same as in the URAT and GRAT methods, selected from a uniform array with a spacing of $\lambda/4$ within the array aperture.

When the array aperture set as 5λ and the MLW constraint is set to be MLW=20°, smaller than the other algorithms. The obtained transmit and receive AFs by the proposed algorithm are shown in Fig. 2, and the two are multiplied to obtain the two-way AF. As shown in Fig. 3(a), the PSLs obtained via the proposed algorithm (running time is 198 s), URAT, GRAT, TWTR, TWCR, and ChebW are -33.89, -30.76, -31.84, -38.69, -44.69, and -36.00 dB, respectively, and the element position of each algorithm is shown in Fig. 3(b). Under the condition that the maximum excitation of the transmit arrays and the Euclidean norm of the receive arrays are specified, the gain of two-way arrays obtained by each algorithm is presented in Table I.

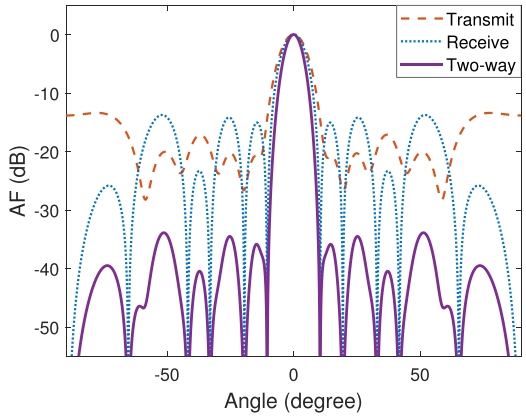

Fig. 2. Obtained transmit and receive AFs by the proposed algorithm with 5λ aperture and MLW=20°.

TABLE I
Gain Obtained by Different Algorithms as 5λ Array Aperture

	Proposed	URAT	GRAT	TWTR	TWCR	ChebW
Transmit gain (dB)	20.83	20.83	20.83	17.50	17.81	19.22
Receive gain (dB)	18.06	18.06	18.06	17.60	19.02	19.34
Total gain (dB)	38.89	38.89	38.89	35.10	36.83	38.56

TABLE II
Position of Transmit Elements (p_m) and Receive Elements (q_n)

m/n	$p_m(\lambda)$	$q_n(\lambda)$	m/n	$p_m(\lambda)$	$q_n(\lambda)$
1	0.00	0.00	9	4.00	6.00
2	0.75	0.75	10	4.50	6.75
3	1.50	1.50	11	4.75	7.50
4	2.25	2.25	12	5.25	-
5	2.50	3.00	13	5.75	-
6	3.00	3.75	14	6.00	-
7	3.25	4.50	15	6.75	-
8	3.75	5.25	16	7.50	-

TABLE III
Gain Obtained by Different Algorithms as 7.5λ Array Aperture

	Proposed	URAT	GRAT	TWTR	TWCR	ChebW
Transmit gain (dB)	24.08	24.08	24.08	20.83	21.36	22.23
Receive gain (dB)	20.83	20.83	20.83	19.37	20.69	20.91
Total gain (dB)	44.91	44.91	44.91	40.20	42.05	43.14

Fig. 3(c) shows the beam-scanning results under the aforementioned constraints; we consider three beams pointing toward $\theta_0 = 5°$, $\theta_0 = 15°$, and $\theta_0 = 25°$, respectively. The obtained PSL is -31.85 dB, a slight improvement occurs due to the widened sidelobe region in the form of a sine value.

The two-way AFs with the aperture size set within 7.5λ while the MLW constraint is set to be MLW=13.6° are compared in Fig. 4(a). The PSLs obtained via the proposed algorithm (running time is 2384 s), URAT, GRAT, TWTR, TWCR, and ChebW are -38.18, -29.82, -31.71, -41.68, -45.84, and -37.00 dB, respectively, and the element position obtained by the proposed algorithm is shown in Fig. 4(b) and is listed in Table II numerically. Table III presents the gain of two-way arrays obtained by each algorithm. It can be found that although the PSLs obtained by TWTR and TWCR are lower, this comes at the cost of a larger MLW and

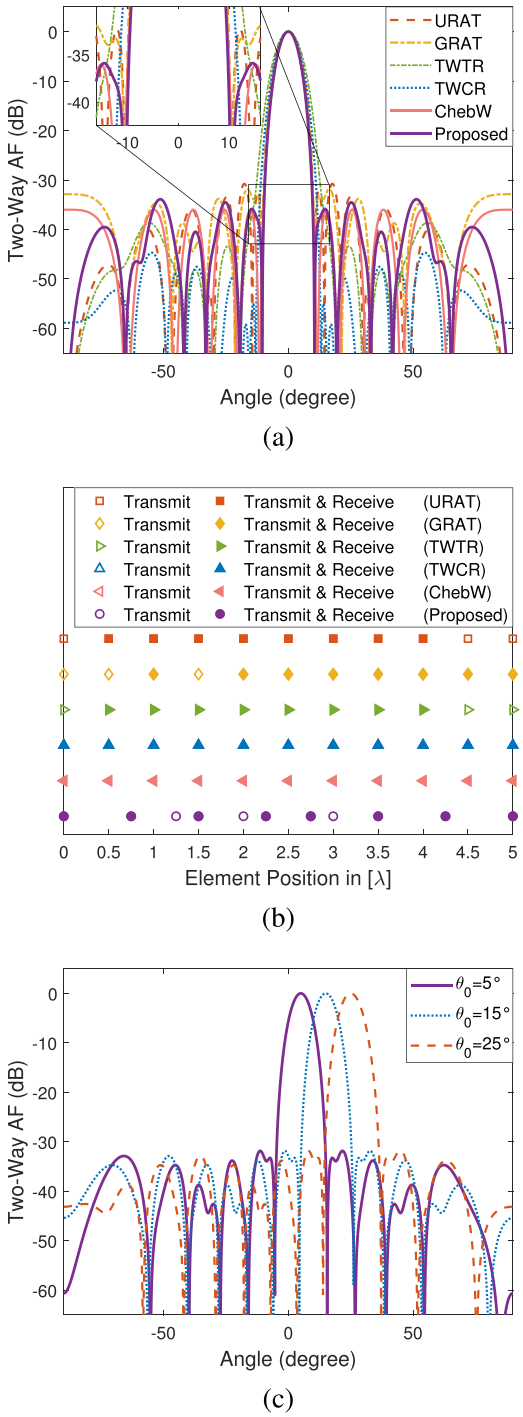

Fig. 3. Two-way AF comparison for PSL minimization as 5λ array aperture. (a) Two-way AFs obtained by different algorithms. (b) Position of transmit elements and receive elements of each algorithm. (c) Beam-scanning results by the proposed algorithm.

complex excitation distribution, while our algorithm can guarantee uniform excitation. It is evident that the proposed algorithm obtains satisfactory PSL and gain with elements work at uniform excitation. For this scenario, we further perform mutual coupling effect and full-wave simulation, the results are generally good as shown in Fig. 4(c), but it can be discovered that the sidelobe level far from the normal direction is slightly elevated in full-wave simulation.

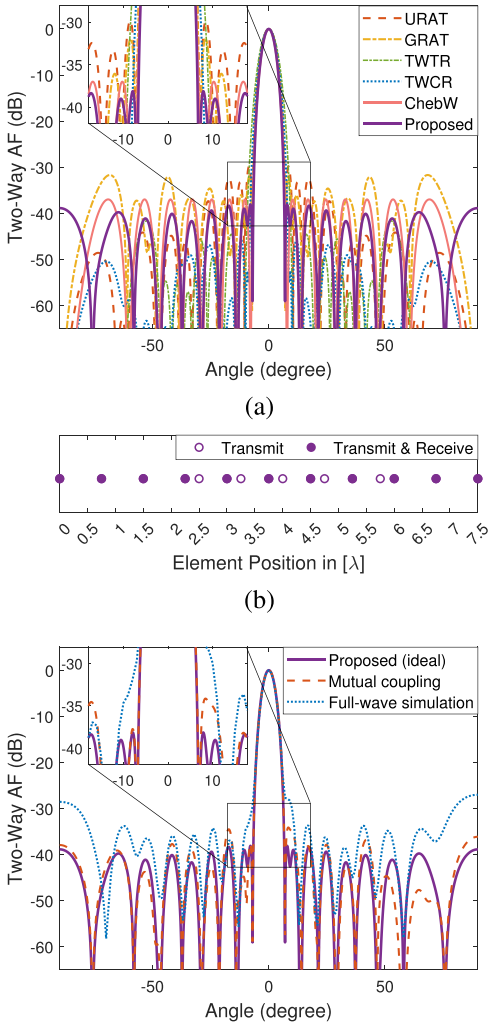

Fig. 4. Two-way AF comparison for PSL minimization as 7.5λ array aperture. (a) Two-way AFs obtained by different algorithms. (b) Position of transmit elements and receive elements obtained by the proposed algorithm. (c) Two-way AF obtained by the proposed algorithm with results of mutual coupling effect and full-wave simulation.

TABLE IV
Resulting PSLs and Running Times Obtained With Various MLW Constraints

	MLW $= 12°$	MLW $= 16°$	MLW $= 20°$	MLW $= 24°$	MLW $= 28°$
PSL (dB)	-16.52	-28.14	-33.89	-35.92	-37.08
Running time (s)	102	41	198	97	29

2) *PSL Minimization With Different MLW:* To evaluate the influence of MLW constraint on two-way AF PSL minimization, consider selecting 11 transmit elements and eight receive elements from 21 uniformly spaced elements with a spacing of $\lambda/4$. In Fig. 5(a), the results of the proposed algorithm under various MLW constraints are presented, and the obtained element position is shown in Fig. 5(b). The resulting PSLs and running times obtained with various MLW constraints are presented in Table IV. It indicates that the MLW can be adjusted as desired utilizing the proposed algorithm.

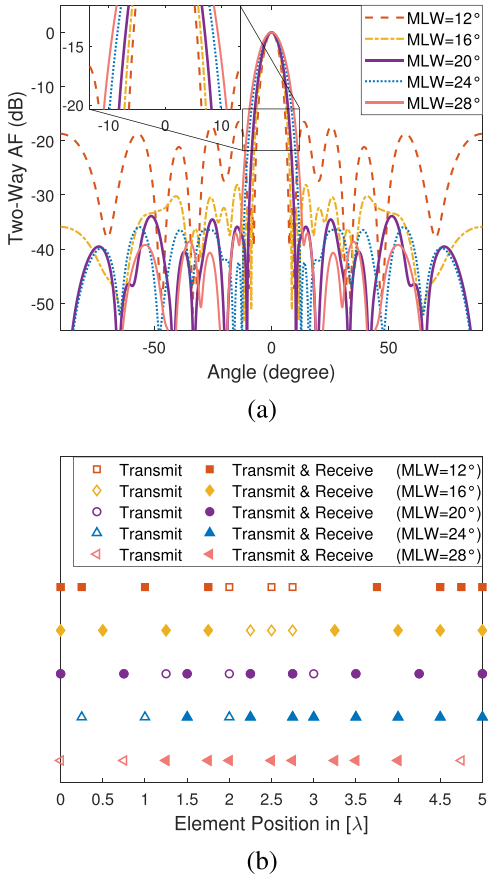

Fig. 5. PSL minimization of two-way AF via the proposed algorithm with different MLW constraints. (a) Two-way AFs obtained with different MLW constraints. (b) Position of transmit elements and receive elements obtained with different MLW constraints.

3) *PSL Minimization With Different N_r:* Consider selecting 11 transmit elements from a linear array comprising 21 uniformly spaced elements with a spacing of $\lambda/4$ and MLW=20°. In Fig. 6(a), the results of the proposed algorithm under various N_r constraints are presented, and the obtained element position is shown in Fig. 6(b). The resulting PSLs and running times obtained with various N_r are shown in Fig. 6(c). It can be seen that the change curve of PSL with N_r does not change monotonically and when the number of elements in receive array is set as $N_r = 9$, the lowest PSL can be achieved. It indicates that the performance of the proposed algorithm can be further optimized by setting the value of N_r.

4) *PSL Minimization in Large-Scale Array:* To examine the performance of the proposed algorithm in a large-scale array, consider selecting 61 transmit elements and 44 receive elements from 121 uniformly spaced elements with a spacing of $\lambda/4$, and the MLW constraint is set to be MLW=3.6°. Fig. 7(a) shows a suboptimal two-way AF obtained after 76 229 s of running time, and it can be observed that the obtained PSL is -40.17 dB. For this scenario, we further perform mutual coupling effect and full-wave simulation; the results are satisfactory as shown. The element position is shown in Fig. 7(b). This proves that the proposed algorithm shows satisfactory performance

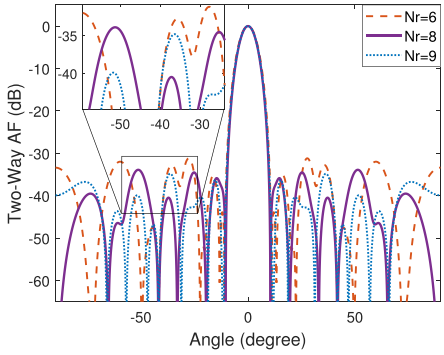

(a)

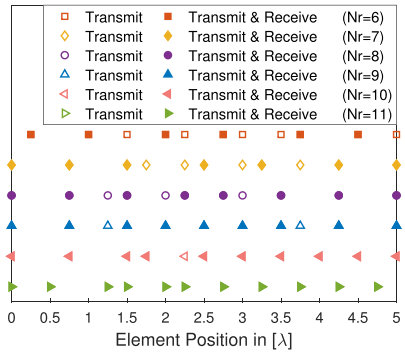

(b)

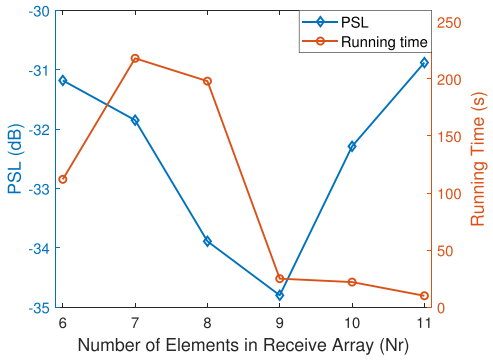

(c)

Fig. 6. PSL minimization of two-way AF via the proposed algorithm with different N_r constraints. (a) Two-way AFs obtained with different N_r constraints. (b) Position of transmit elements and receive elements obtained with different N_r constraints. (c) Resulting PSLs and running times obtained with different N_r constraints.

in a large-scale array, and suboptimal solutions can be considered to reduce running time.

B. Minimize the Number of Transmit Elements

In the second example, we perform simulations of the scenario that minimizes the number of transmit elements with a determined PSL constraint.

1) *Two-Way AF Comparison:* Various algorithms are simulated to study the performance of the proposed algorithm for minimizing the number of transmit elements. Consider the scenario as the array aperture size set within 7λ. According to the simulation result of the URAT method, the number of transmit elements is 15 and the obtained MLW

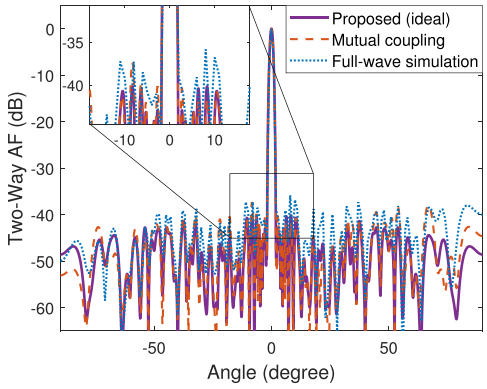

(a)

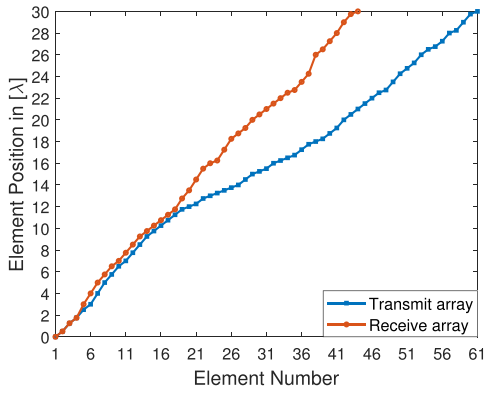

(b)

Fig. 7. PSL minimization of two-way AF via the proposed algorithm in large-scale array. (a) Two-way AF obtained with results of mutual coupling effect and full-wave simulation. (b) Position of transmit elements and receive elements obtained.

of the resulting two-way AF is 14.2°. The PSL obtained by the GRAT method is -32.77 dB with the same MLW.

The above data are generated as constraints of the proposed algorithm, and elements are selected from a uniform array with a spacing of λ/4 . In Fig. 8(a), the resulting two-way AF obtained by each method is shown. After 1323 s of running time, the obtained number of transmit elements is 12, and due to the discontinuity of the selected position and weight of the elements, the obtained PSL of the resulting two-way AF is -33.33 dB, lower than the constraint. For this scenario, we further perform full-wave simulation, and the result is satisfactory as shown. The position of elements obtained by the proposed algorithm is shown in Fig. 8(b). The simulations show that a smaller number of transmit elements can be selected to achieve more satisfactory two-way AF via the proposed algorithm.

2) *Minimize the Number of Transmit Elements With Different PSLs:* Consider a uniform array comprising 21 elements with a spacing of λ/4. The MLW constraint is set as MLW=20°. To evaluate the influence of PSL constraint on two-way AF, the results of the proposed algorithm under various PSL constraints are shown in Fig. 9(a), and the obtained position of elements is shown in Fig. 9(b). The resulting number of transmit elements (i.e., N_t) and running

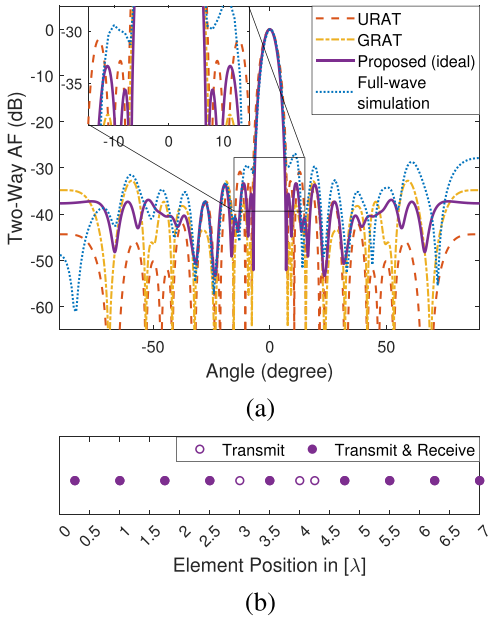

Fig. 8. Two-way AF comparison for minimizing the number of transmit elements as 7λ array aperture. (a) Two-way AFs obtained by different algorithms and full-wave simulation result of the proposed algorithm. (b) Position of transmit elements and receive elements obtained by the proposed algorithm.

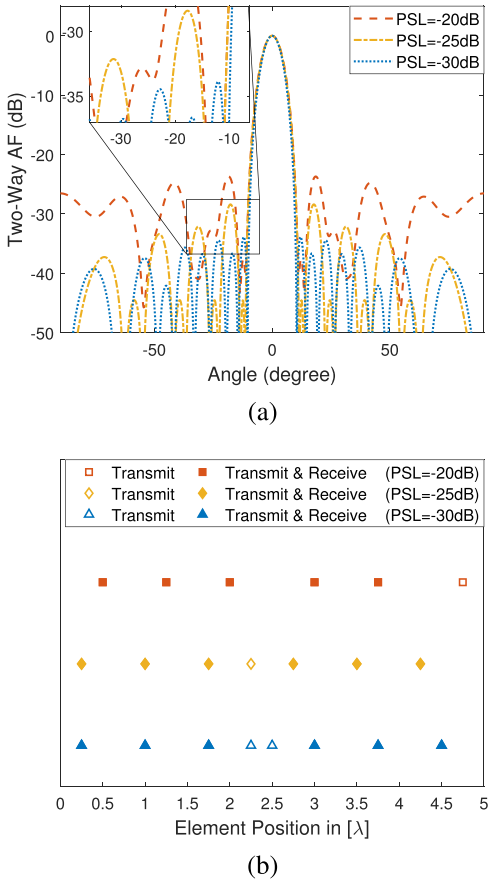

Fig. 9. Minimize the number of transmit elements of two-way array via the proposed algorithm with different PSL constraints. (a) Two-way AFs obtained with different PSL constraints. (b) Position of transmit elements and receive elements obtained with different PSL constraints.

TABLE V
Resulting N_t and Running Times Obtained With Various PSL Constraints

	PSL =-20dB	PSL =-25dB	PSL =-30dB
N_t	6	7	8
Running time (s)	241	202	102

TABLE VI
Resulting Min-Spacing and Running Times Obtained With Various PSL Constraints

	PSL =-20dB	PSL =-25dB	PSL =-30dB
Min-spacing	$3\lambda/4$	$3\lambda/4$	$\lambda/2$
Running time (s)	18	147	115

times obtained with various PSL constraints are presented in Table V. It is worth noting that the obtained PSLs of the resulting two-way AFs are -23.69, -28.39, and -33.86 dB, respectively, lower than the constraint. It indicates the effectiveness of the proposed algorithm in element number minimization.

C. Maximize the Min-Spacing Between Transmit Elements

In the third example, we perform simulations of the scenario that maximizes the min-spacing between transmit elements with determined PSL constraint.

1) *Two-Way AF Comparison:* Various algorithms are simulated to study the performance of the proposed algorithm for maximizing the min-spacing between transmit elements. Consider the scenario as the array aperture size set within 6λ. According to the simulation result of the URAT method, the element spacing is $\lambda/2$ and the obtained MLW of the resulting two-way AF is 16.0°. The PSL obtained by the GRAT method is -30.27 dB with the same MLW.

The above data are generated as constraints of the proposed algorithm, and elements are selected from a uniform array with a spacing of $\lambda/6$. In Fig. 10(a), the resulting two-way AFs obtained by the proposed algorithm and the RAT method are shown. After 1851 s of running time, the obtained min-spacing between transmit elements is $2\lambda/3$, and the obtained PSL of the resulting two-way AF is -30.30 dB, lower than the constraint. For this scenario, we further perform full-wave simulation; the result is generally good as shown, but it can be discovered that the sidelobe level far from the normal direction is slightly elevated. The position of elements obtained by the proposed algorithm is shown in Fig. 10(b). The simulations show that larger min-spacing between transmit elements can be generated to achieve more satisfactory two-way AF via the proposed algorithm.

2) *Maximize the Min-Spacing Between Transmit Elements With Different PSLs:* Consider a uniform array comprising 21 elements with a spacing of $\lambda/4$. The MLW constraint is set as MLW=20°. To evaluate the influence of PSL constraint on two-way AF, the results of the proposed algorithm under various PSL constraints are shown in Fig. 11(a), and the obtained position of elements is shown in Fig. 11(b).

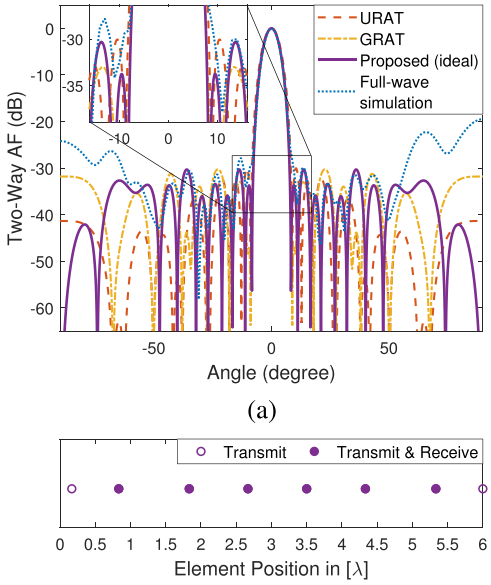

(a)

(b)

Fig. 10. Two-way AF comparison for maximizing the min-spacing between transmit elements as 6λ array aperture. (a) Two-way AFs obtained by different algorithms and full-wave simulation result of the proposed algorithm. (b) Position of transmit elements and receive elements obtained by the proposed algorithm.

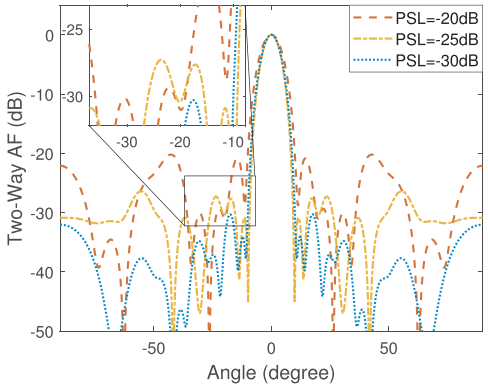

(a)

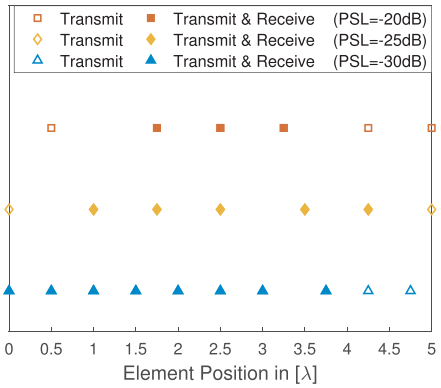

(b)

Fig. 11. Maximize the min-spacing between transmit elements of two-way array via the proposed algorithm with different PSL constraints. (a) Two-way AFs obtained with different PSL constraints. (b) Position of transmit elements and receive elements obtained with different PSL constraints.

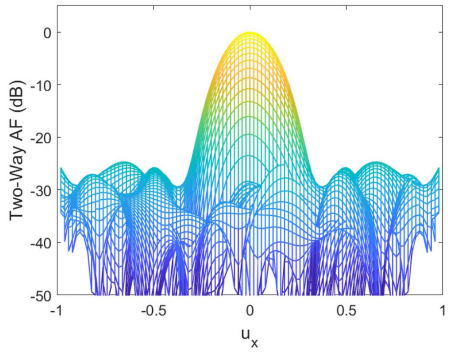

(a)

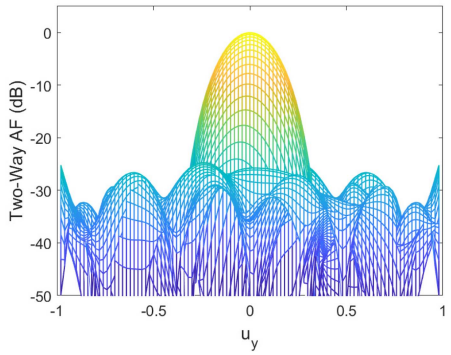

(b)

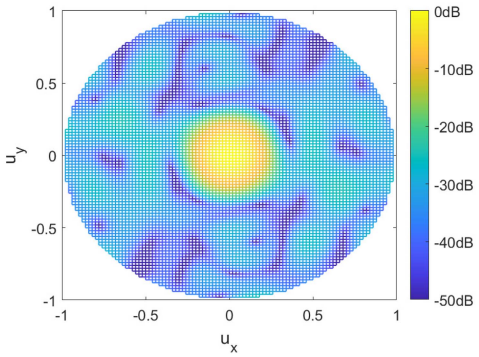

(c)

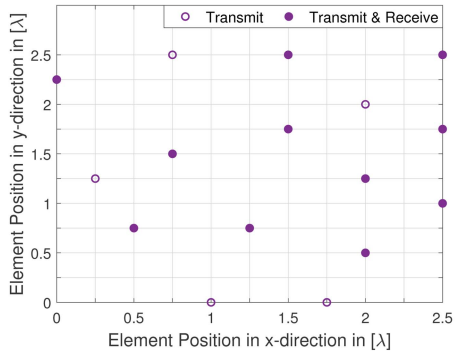

(d)

Fig. 12. Maximize the min-spacing between transmit elements in planar array. (a) Two-way AF obtained by the proposed algorithm viewed in u_x-direction. (b) Two-way AF obtained by the proposed algorithm viewed in u_y-direction. (c) Two-way AF obtained by the proposed algorithm viewed in u_x-u_y direction. (d) Position of transmit elements and receive elements obtained by the proposed algorithm.

The resulting min-spacing and running times obtained with various PSL constraints are presented in Table VI. It is worth noting that the obtained PSLs of the resulting two-way AFs are -20.22, -26.41, and -30.30 dB, respectively, lower than the constraint. It indicates the effectiveness of the proposed algorithm in min-spacing maximization.

3) *Maximize the Min-Spacing Between Transmit Elements in Planar Array:* To validate the performance of the proposed algorithm in a planar array, consider the scenario as the array aperture size set within $2.5\lambda \times 2.5\lambda$. The sidelobe region of the two-way AF is set as ${u_x}^2 + {u_y}^2 \geq 0.35^2$, where $u_x = \sin\phi\cos\theta$ while $u_y = \sin\phi\sin\theta$, and ϕ stands for the polar angle. The PSL is constrained to below -25.00 dB. The elements are selected from a uniform planar array with spacing both $\lambda/4$ in x- and y-directions. The resulting two-way AF viewed in various directions and the obtained position of transmit elements and receive elements are shown in Fig. 12. After 15 303 s of running time, the obtained min-spacing between transmit elements is $\sqrt{5}\lambda/4$. It indicates that the proposed algorithm can be applied to the planar array and effectively increase the min-spacing between transmit elements.

VI. CONCLUSION

In this article, we have proposed a novel approach for two-way array synthesis with low sidelobe level via MIP. The proposed algorithm optimizes element positions of the two-way array to suppress the PSL utilizing integer modeling techniques. Our algorithm is applicable to different scenarios, such as PSL minimization, element number minimization, and element min-spacing maximization. For each scenario, we formulated different MIP models that can be solved using off-the-shelf solvers. The effectiveness and ease of implementation of our algorithm in PSL suppression have been proved. Representative simulations are provided to demonstrate the effectiveness and superiority of the proposed algorithm.

REFERENCES

[1] P. Z. Peebles, *Radar Principles*. Hoboken, NJ, USA: Wiley, 2007.

[2] G. T. F. D. Abreu and R. Kohno, "A modified Dolph–Chebyshev approach for the synthesis of low sidelobe beampatterns with adjustable beamwidth," *IEEE Trans. Antennas Propag.*, vol. 51, no. 10, pp. 3014–3017, Oct. 2003.

[3] A. Villeneuve, "Taylor patterns for discrete arrays," *IEEE Trans. Antennas Propag.*, vol. AP-32, no. 10, pp. 1089–1093, Oct. 1984.

[4] J. F. DeFord and O. P. Gandhi, "Phase-only synthesis of minimum peak sidelobe patterns for linear and planar arrays," *IEEE Trans. Antennas Propag.*, vol. 36, no. 2, pp. 191–201, Feb. 1988.

[5] Y. Aslan, J. Puskely, A. Roederer, and A. Yarovoy, "Phase-only control of peak sidelobe level and pattern nulls using iterative phase perturbations," *IEEE Antennas Wireless Propag. Lett.*, vol. 18, no. 10, pp. 2081–2085, Oct. 2019.

[6] W. Zhang, L. Li, and F. Li, "Reducing the number of elements in linear and planar antenna arrays with sparseness constrained optimization," *IEEE Trans. Antennas Propag.*, vol. 59, no. 8, pp. 3106–3111, Aug. 2011.

[7] C. Zhang, X. Fu, L. Leo, S. Peng, and M. Xie, "Synthesis of broadside linear aperiodic arrays with sidelobe suppression and null steering using whale optimization algorithm," *IEEE Antennas Wireless Propag. Lett.*, vol. 17, no. 2, pp. 347–350, Feb. 2018.

[8] S. K. Goudos, K. Siakavara, T. Samaras, E. E. Vafiadis, and J. N. Sahalos, "Sparse linear array synthesis with multiple constraints using differential evolution with strategy adaptation," *IEEE Antennas Wireless Propag. Lett.*, vol. 10, pp. 670–673, 2011.

[9] B. Fuchs, A. Skrivervik, and J. R. Mosig, "Synthesis of uniform amplitude focused beam arrays," *IEEE Antennas Wireless Propag. Lett.*, vol. 11, pp. 1178–1181, 2012.

[10] D. Pinchera, M. D. Migliore, and G. Panariello, "Synthesis of large sparse arrays using IDEA (inflating-deflating exploration algorithm)," *IEEE Trans. Antennas Propag.*, vol. 66, no. 9, pp. 4658–4668, Sep. 2018.

[11] R. L. Haupt, "Thinned arrays using genetic algorithms," *IEEE Trans. Antennas Propag.*, vol. 42, no. 7, pp. 993–999, Jul. 1994.

[12] O. Quevedo-Teruel and E. Rajo-Iglesias, "Ant colony optimization in thinned array synthesis with minimum sidelobe level," *IEEE Antennas Wireless Propag. Lett.*, vol. 5, pp. 349–352, 2006.

[13] X. K. Wang, Y. C. Jiao, and Y. Y. Tan, "Synthesis of large thinned planar arrays using a modified iterative Fourier technique," *IEEE Trans. Antennas Propag.*, vol. 62, no. 4, pp. 1564–1571, Apr. 2014.

[14] A. J. Abdulqader, J. R. Mohammed, and R. H. Thaher, "Phase-only nulling with limited number of controllable elements," *Prog. In Electromagn. Res. C.*, vol. 99, pp. 167–178, 2020.

[15] J. R. Mohammed, A. J. Abdulqader, and R. H. Thaher, "Antenna pattern optimization via clustered arrays," *Prog. Electromagn. Res. M.*, vol. 95, pp. 177–187, 2020.

[16] J. R. Mohammed, R. H. Thaher, and A. J. Abdulqader, "Linear and planar array pattern nulling via compressed sensing," *J. Telecommun. Inf. Technol.*., vol. 3, pp. 50–55, 2021.

[17] F. L. Anderson, "Two-way beam patterns from ultrawideband arrays," *Proc. SPIE.*, vol. 1631, pp. 25–35, 1992.

[18] N. Ferre, P. Combes, and T. Dusseux, "Transmit-receive optimized patterns for space radar active antennas," in *Proc. 1994 IEEE Antennas Propag. Soc. Int. Symp. URSI Nat. Radio Sci. Meeting.*, 1994, pp. 1240–1243.

[19] M. A. Jensen and J. W. Wallace, "A review of antennas and propagation for MIMO wireless communications," *IEEE Trans. Antennas Propag.*, vol. 52, no. 11, pp. 2810–2824, Nov. 2004.

[20] H. Y. Lu and W. H. Fang, "Joint transmit/receive antenna selection in MIMO systems based on the priority-based genetic algorithm," *IEEE Antennas Wireless Propag. Lett.*, vol. 6, pp. 588–591, 2007.

[21] C. X. Mao, S. Gao, and Y. Wang, "Dual-band full-duplex Tx/Rx antennas for vehicular communications," *IEEE Trans. Veh. Technol.*, vol. 67, no. 5, pp. 4059–4070, May 2018.

[22] V. Towhidlou and M. Shikh-Bahaei, "Adaptive full-duplex communications in cognitive radio networks," *IEEE Trans. Veh. Technol.*, vol. 67, no. 9, pp. 8386–8395, Sep. 2018.

[23] B. C. Brock, "The application of Taylor weighting, digital phase shifters, and digital attenuators to phased-array antennas," Sandia Nat. Lab., Albuquerque, NM, USA, and Livermore, CA, USA, Tech. Rep. SAND2008-1687, 2008.

[24] J. N. Sahalos, "Design of shared aperture radar arrays with low sidelobe level of the two-way array factor," *IEEE Trans. Antennas Propag.*, vol. 68, no. 7, pp. 5415–5420, Jul. 2020.

[25] J. N. Sahalos, "Lowering the sidelobe level of a two-way pattern in shared aperture radar arrays," *Int. J. Antennas Propag.*, vol. 2021, pp. 1–10, 2021.

[26] T. Samaras and J. Sahalos, "A systematic study of low SLL two-way pattern in shared aperture radar arrays," *Prog. Electromagn. Res. C.*, vol. 128, pp. 169–182, 2023.

[27] R. Rajender, K. R. Subhashini, and B. P. Kumar, "Two-way array factor supported by thinning strategy for an improved radar performance," in *Proc. Nat. Conf. Commun.*, 2021, pp. 1–4.

[28] R. Rajender, S. Choudhury, K. R. Subhashini, G. Ciarpi, S. Genovesi, and D. Rossi, "Design of linear and planar arrays with low sidelobe levels and high directivity using two-way array factor," *IEEE Trans. Antennas Propag.*, vol. 72, no. 5, pp. 4150–4160, May 2024.

[29] T. N. F. Kaifas and J. N. Sahalos, "Low SLL control of two-way pattern in shared circular planar radar arrays," *IEEE Trans. Antennas Propag.*, vol. 72, no. 3, pp. 2915–2920, Mar. 2024.

[30] R. L. Haupt and P. Nayeri, "Uniform arrays with low sidelobe two-way antenna patterns," in *Proc. IEEE 12th Eur. Conf. Antennas Propag.*, 2018, pp. 1–2.
[31] R. L. Haupt, "Lowering the sidelobe level of a two-way array factor for an array with uniform transmit and uniform receive arrays," *IEEE Trans. Antennas Propag.*, vol. 67, no. 6, pp. 4253–4256, Jun. 2019.
[32] J. Wang, X. Wu, J. Ye, J. Sun, and G. Hua, "A novel two-way pattern synthesis method with the uniform and thinned arrays," *IEEE Antennas Wireless Propag. Lett.*, vol. 23, no. 10, pp. 3108–3112, Oct. 2024.
[33] R. L. Haupt, "Optimizing the sidelobe level of a two-way antenna array pattern by thinning the receive aperture," in *Proc. Int. Conf. Radar.*, 2018, pp. 1–5.
[34] E. Loew and R. L. Haupt, "Two-way pattern synthesis for the airborne phased array radar (APAR)," in *Proc. 2022 IEEE Int. Symp. Phased Array Syst. Technol.*, 2022, pp. 1–3.
[35] Gurobi Optimization, *Gurobi Optimizer Reference Manual*, Dallas, TX, USA: Briarwood, 2023.
[36] IBM ILOG CPLEX, *Optimization Studio CPLEX Users Manual*. Raleigh, NC, USA: IBM, 2018.
[37] X. Zhang, Z. He, X. Zhang, and J. Xie, "Robust sidelobe control via complex-coefficient weight vector orthogonal decomposition," *IEEE Trans. Antennas Propag.*, vol. 67, no. 8, pp. 5411–5425, Aug. 2019.